Powder Technology 338 (2018) 173–179

Contents lists available at ScienceDirect

Powder Technology

journal homepage: www.elsevier.com/locate/powtec

Modification of cryomilling process to tailor geometrical characteristics of nanostructured Al powder for cold spraying

Bo Feng [a,b], Naeem ul Haq Tariq [a,b,d], Jiqiang Wang [a,*], Hao Du [a], Xusheng Zang [a,c], Tianying Xiong [a,*]

[a] Institute of Metal Research, Chinese Academy of Sciences, Shenyang 110016, PR China
[b] University of Chinese Academy of Science, No. 19 (A) Yuquan Road, Shijingshan District, Beijing 100049, PR China
[c] School of Materials Science and Engineering, University of Science and Technology of China, Shenyang 110016, PR China
[d] Department of Metallurgy and Materials Engineering, Pakistan Institute of Engineering and Applied Sciences, Nilore, Islamabad, Pakistan

ARTICLE INFO

Article history:
Received 18 April 2018
Received in revised form 16 June 2018
Accepted 4 July 2018
Available online 6 July 2018

Keywords:
Cryomilling
Cold spraying
Nanostructured Al powder
Powder morphology
Powder size distribution

ABSTRACT

Cryomilling is the most commonly used method to fabricate ultra-fine grained (UFG) or nanostructured metallic powder. However, it has relatively low control over powder's geometric characteristics, particularly for the powders having FCC crystal structure. This shortcoming makes traditional cryomilling process unattractive to produce UFG/nanostructured feedstock for cold spraying process. In the present work, a modified pot vibration milling process was successfully employed to produce nanostructured powder of pure aluminum at 100 K. The geometrical characteristics of Al powder was controlled by using various combinations of the milling media (i.e. steel balls) of different sizes. The results indicate that with increase in milling time, the initial grain size of Al (~1–5 μm) was progressively refined to ~30–50 nm. Moreover, lamellar powder morphology was obtained with the addition of process control agent (PCA) while equiaxed polygonal structure was evolved without using PCA. It was also revealed that, in the absence of PCA, the particle size distribution was mainly controlled by the interstice size distribution of the milling media.

1. Introduction

Nano technology is the foundation of modern material science and engineering. In early 1980s, H. Gleiter first proposed the concept of nanostructured material [1]. Materials at nanometer length scale may exhibit physical properties that are entirely different from the characteristics of their bulk state [2]. In bulk nanostructured materials, the grain refinement usually leads to superior mechanical and physical properties as compared to their coarse-grained counterparts [3–5].

In powder metallurgy, high-energy milling of the powder followed by a consolidation process is the most commonly used method to prepare nanostructured materials. The fabrication of nanostructured powder by high-energy milling has some advantages over other powder processing methods, e.g. high output, flexibility of the process and simplicity of the equipment. For the past three decades, this area has attained a great attention of the researchers [6,7]. However, many studies show that due to the structural features of FCC materials, it is very difficult to form nano-crystalline structure at room temperature due to undesired recovery (RV) and recrystallization (RX) phenomena.

Cryomilling is a mechanical attrition technique in which powders are milled at very low temperature, which usually depend on the liquid nitrogen (LN2) refrigeration process. At cryogenic temperature (~100 K) RV and RX processes become extremely sluggish while dispersed metal nitrides are formed in the milled powder. As a result, nano-crystallization of FCC powder material is facilitated [8,9]. Meanwhile, the powder fabricated by this method has relatively high strength and high thermal stability [9]. In the past, this technique was used to produce nanocrystalline powder of Fe—Al, Ni—Al intermetallic compounds [10–12], M50 steel [13] and Fe based metglas [14]. Later, a wave of research, focusing on the preparation of nanostructured powder of pure Al, Al alloy and Al-MMCs, was emerged [8,15–19]. For pure Al and Al alloys, the existing powder consolidation technologies include some conventional powder metallurgy techniques, such as HIP [19,20], hot rolling [21], spark plasma sintering [22], vacuum hot pressing, etc. [23,24]. However, these consolidation technologies often affect the final structure of the powder due to high processing temperature.

Cold spraying (CS) is an emerging solid-state additive manufacturing technology, which mainly depends on the powerful kinetic energy of the impacting particles to achieve the coherence between the powder particles. The low-temperature solid-state processing makes CS an attractive technique to spray thermally sensitive materials, such as nanostructured, amorphous materials etc. [25]. Nearly a decade ago, Ajdelsztajn et al. first used cryomilled feedstock powder to prepare nanostructured coating through CS [26,27]. Later on, many researchers carried out the follow-up studies on pure Al [28], Aluminum alloy

* Corresponding authors.
E-mail addresses: jqwang11s@imr.ac.cn, (J. Wang), tyxiong@imr.ac.cn (T. Xiong).

https://doi.org/10.1016/j.powtec.2018.07.007
0032-5910/

2009 [29], Aluminum alloy 2618 [30], Aluminum alloy 5083 [26,31,32], Al-7.6 at.% Mg [33], Aluminum alloy 6061 [31], Aluminum alloy 7075 [34], B_4C-Al12Si MMCs [35], CNT-Al MMCs [36] etc. These studies demonstrate successful fabrication of the nanostructured coatings that retain the inherent structural features of the feedstock powder. The coatings exhibited ultra-high hardness, along with increased porosity compared with the coatings fabricated by gas atomization powder.

In CS, kinetic energy is transferred to powder particles from the supersonic gas stream coming from the converging-diverging type gun nozzle. Therefore, the kinetic energy storage capacity of the powder is of the paramount importance which influences the quality of the deposit to a great extent. This capacity depends upon the density, size distribution and morphology of the starting powder. Meanwhile, an optimal size distribution range is required for different kind of powders to achieve high deposition efficiency during CS. Many factors influence the optimal size distribution for a powder. These include; density of the particles, their deformability, and the thickness of surface oxide film of the starting powder. Therefore, it is imperative to carefully tailor the morphology and size distribution of the feedstock powder to suit CS process. Unfortunately, traditional cryomilling operation has relatively low control over powder's geometric characteristic, particularly for the powders having FCC crystal structure. This shortcoming makes this process unattractive to produce UFG/nanostructured feedstock for cold spraying process.

In past, no serious attention was paid to the morphology of cryomilled feed stock powder. Consequently, benefits associated with the cold spraying process could not be achieved completely. For instance, the morphology of the starting pure Al powder is completely changed from spherical to lamellar structure as a result of traditional cryomilling process. This kind of powder morphology is not suitable for CS process to achieve high deposition efficiency and good tamping effect. Therefore, the present study was carried out with the aim to explore the influence of cryomilling process on geometrical characteristics and grain refinement of pure Al powder at various milling conditions. The geometrical characteristics of Al powder was controlled by using various combinations of the milling media (i.e. steel balls) of different sizes.

2. Material and methods

Commercially available atomized pure Al powder with particle size <20 μm (~600 mesh) was milled in a modified pot vibration mill with stainless steel balls. Nanocrystalline Al powder was successfully produced by cryomilling at 100 K. The vibration frequency and the amplitude for the milling process were kept at 45 Hz and 5 mm, respectively. Seven different sizes of stainless steel balls and as-atomized stainless steel powders were used as the milling media. The balls were designated as D_{10}, D_7, D_5, D_1, $D_{0.5}$ $D_{0.3}$ $D_{0.1}$, whereas the subscript shows the diameter of the ball in millimeter. The other parameters of the milling process are summarized in Table 1.

The size distribution of various powders was made using Malvern mastersizer 2000. The morphology of the powders was observed by FEI Inspect F scanning electron microscopy (SEM). Transmission electron microscopy (TEM) was performed using 200 kV FEI Tecnai F20 equipment. Microhardness measurements were performed on the cross-section of different powders using a Vickers microhardness tester (AMH43, Leco, USA) under a 10 g load and 15 s holding time. For each powder sample, at least 7 indentations were taken at random locations and their average values as well as the standard deviation were calculated.

3. Results

The SEM micrograph of the as-received Al powder is shown in Fig. 1. The as-atomized powder shows uniform equiaxed spheres with smooth surface morphology.

3.1. Properties of the cryomilled powders

The SEM micrographs of Al powder cryomilled at different milling conditions (in the presence of PCA) are shown in Fig. 2. It can be observed that by adding PCA in the vibration mill, the cold welding of the particles is completely inhibited. Under cryomilling conditions, powder particles experienced severe deformation due to the repeated

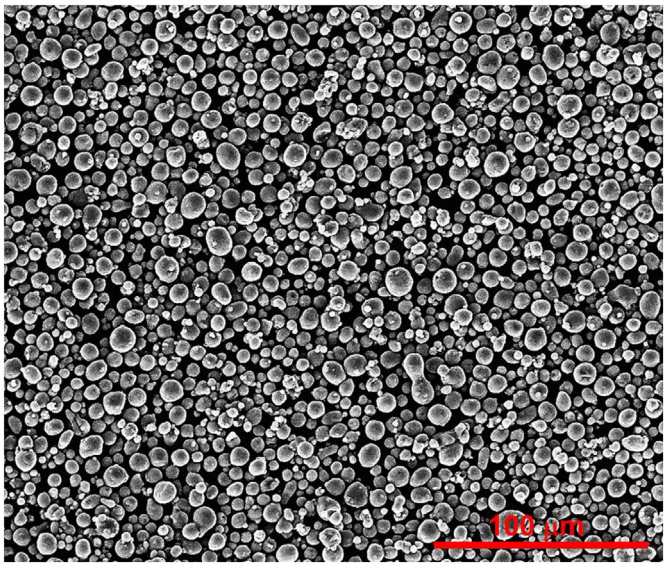

Fig. 1. SEM image of as-received Al powder.

Table 1
Summary of different parameters for modified vibratory milling process.

Powder designation	PCA (Stearic acid, wt%)	Milling time (hr)	Milling balls		Ball-to-powder weight ratio	Filling ratio (%)
			Combination	Dissimilar balls weight ratio		
1–1	5	2				
1–2	5	4				
1–3	5	7				
1–4	5	13	D_{10}, D_7, D_5	1:1:1	15:1	60
1–5	1	4				
1–6	0.5	4				
1–7	0.1	4				
2–1		2	D_{10}, D_7, D_5	1:1:1		
2–2		2	D_{10}, D_7, D_5, D_1	1:1:1:1		
2–3	–	2	D_{10}, D_7, D_5, $D_{0.5}$	1:1:1:1		
2–4		2	D_{10}, D_7, D_5, $D_{0.3}$	1:1:1:1		
2–5		2	D_{10}, D_7, D_5, $D_{0.1}$	1:1:1:1		

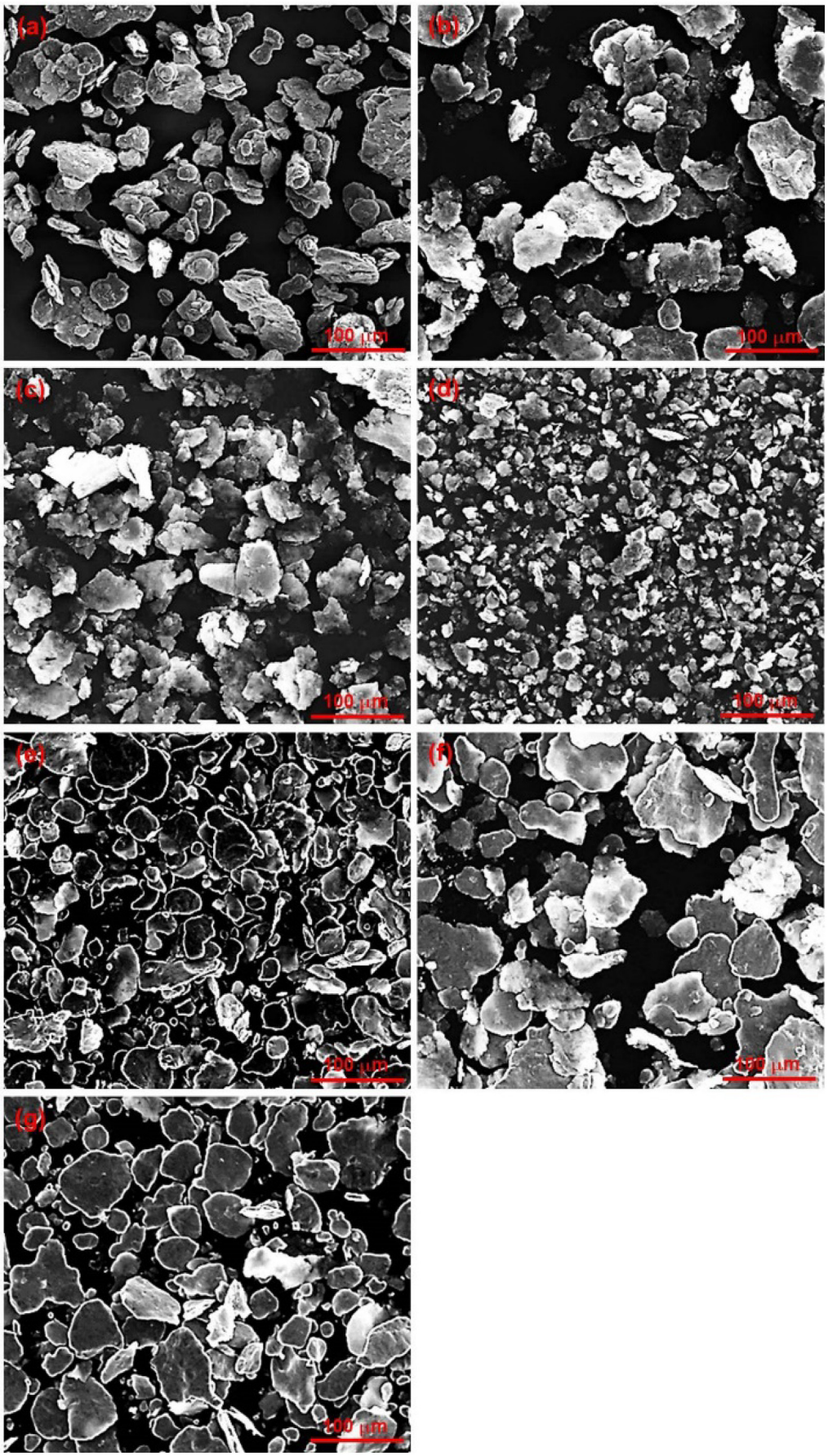

Fig. 2. SEM images of different powders cryo-milled with PCA: (a) powder 1–1, (b) powder 1–2, (c) powder 1–3, (d) powder 1–4, (e) powder 1–5, (f) powder 1–6 and (g) powder 1–7.

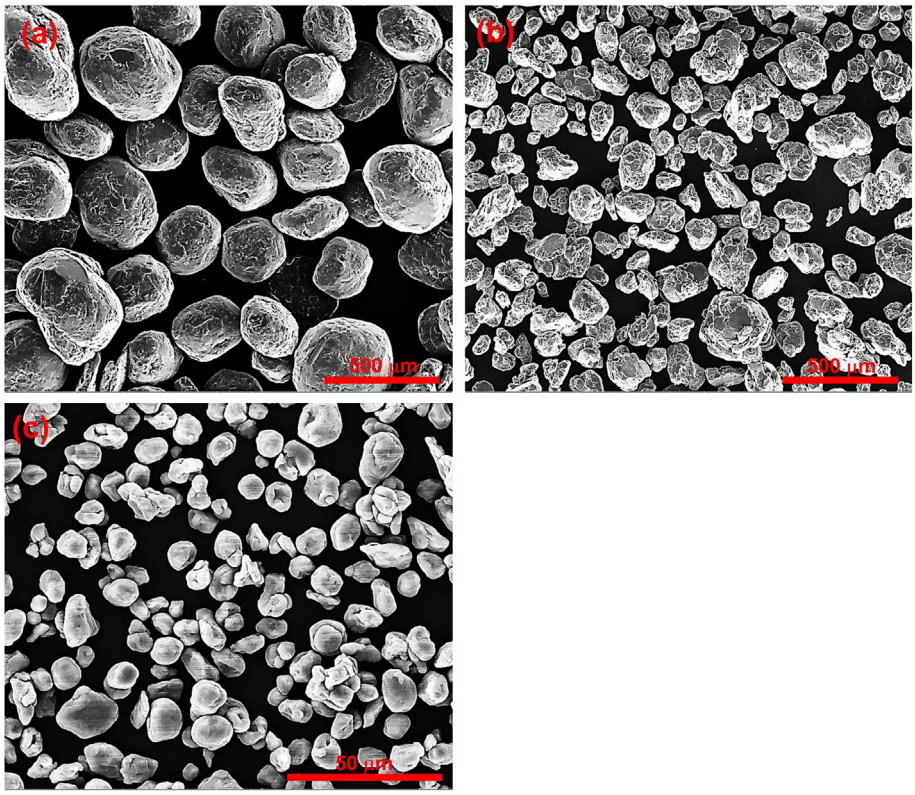

Fig. 3. SEM images of different powders cryo-milled without PCA: (a) powder 2–1, (b) powder 2–3 and (c) powder 2–5.

collision by grinding media. Consequently, the spherical morphology of the starting powder is changed to the lamellar structure. Furthermore, the average thickness of the powders 1–1, 1–2, 1–3 and 1–4 become <100 nm. The thickness of the powder 1–4 is in the range of 30–50 nm. As the milling time was increased, the milling process resulted in the fragmentation of the powder particles, while the thickness of the powder gradually reduced. Quite interestingly, no significant change in the morphology of the powders is observed when the amount of PCA was gradually decreased.

The SEM micrograph of the cryomilled Al powder, in the case when no PCA was used in the pot, is shown in Fig. 3. Due to large plastic deformation, the morphology of the powder is significantly changed. Compared with the spherical morphology of the as-received powder, cryomilled powder changes into irregular polygons with beveled edges. The morphology of the powder is predominantly composed of equiaxed polygonal structures. In addition, few particles with plate-like morphology are also observed.

Cryomilling of Al powder in the presence of PCA resulted in large amount of dislocations which were continuously generated by the severe deformation of the particles, (Fig. 4(a)). Fig. 4(b and c) are the TEM images of the cryomilled powder processed without using PCA. In this case, an equiaxed grain structure was achieved which seems to be formed by the repeated cold welding of the lamellar powder particles. The thickness of these extremely flattened particles (as marked by green lines in Fig. 4(b)) is measured to be ~100–50 nm. To provide more clarity about the nanostructure formation in Al powder, a dark field image (of the same area) is shown in Fig. 4(c).

3.2. Effect of grinding media size on the morphology of the powder

All powders cryomilled without using PCA showed narrow size distribution compared with commercially available atomized Al powder. Laser particle size analysis revealed a relationship between size distribution of cryomilled powder and size of grinding media in the case

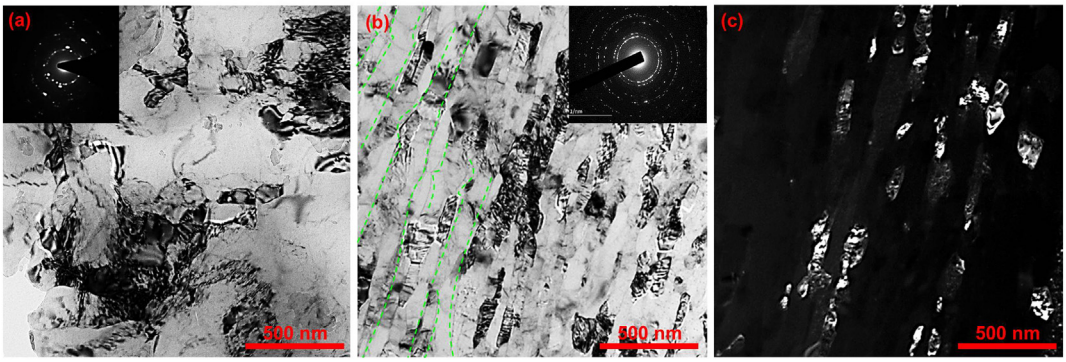

Fig. 4. TEM images of cryomilled powders: (a) bright field image of powder 1–1, (b) bright field image of powder 2–5, (c) dark field image of powder 2–5. The insets in panel (a) and (b) show corresponding SAED patterns.

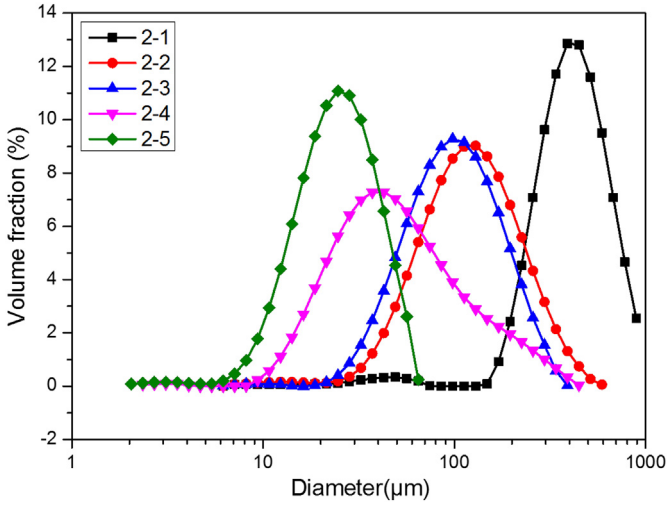

Fig. 5. Particle size distribution of cryomilled powder without using PCA.

when PCA was not used in the milling pot (Fig. 5). By widening the size distribution of the smaller milling media (i.e. by using the balls with diameter < 5 mm), the powder size was gradually decreased. In other words, size distribution of the powder has a direct relationship with the grinding media of minimum diameter.

However, when the minimum diameter of the grinding media is decreased to 100 μm, the d_{50} of the powder 2–5 was reduced to 30 μm. Since smaller grinding media has more specific surface area which results in increased ball to ball and ball to pot frictional forces. Consequently, the repeated impact process becomes less intensive, which in turn results in insufficient deformation of the powder. Therefore, the degree of nano-crystallization in powder 2–5 is comparatively lower than that of the others powders, milled for similar duration. This was further confirmed by measuring the micro-hardness of the milled powders. It was revealed that, by increasing the content of smaller grinding media; the micro-hardness ($HV_{0.01}$) value of the powders was decreased from 70 ± 5 (for powder 2–1) to 45 ± 5 (for powder 2–5). This decrease in the hardness value of powder 2–5 is also in a good agreement with the frictional phenomenon discussed above. Nevertheless, the hardness value of powder 2–5 (45 ± 5) is still much higher than that of the as-received Al powder (25 ± 5), indicating significant microstructural refinement in power 2–5.

4. Discussion

4.1. Morphology of powders

The main mechanism of the vibration mill is associated with the high frequency of the pot. In the milling pot, Al powder undergoes impact twice due to vibratory mode of the milling pot. Firstly, when the powder is located in the middle of two grinding media, the powder particle experiences a uniaxial compression and is severely deformed into the lamellar structure or even broken down into the fragments (Fig. 2(d)). This is the main process of grain refinement and the first powder fragmentation mechanism, (Fig. 6(a)). Secondly, when the powder particles, located in the interstices formed by the grinding media, they experience hydrostatic pressure. Therefore, the powder is compressed hydrostatically. During this process, the powder particles are cold welded together and get compacted. If the size of powder is bigger than that of the interstice, especially bigger than that of the minimum size interstice in a plane (MSIP, formed by the common tangents of the three smallest ball, as shown in Fig. 6(b)), the powder is broken down into small particles due to intense compressive forces. This could be considered as the second mechanism of powder fragmentation.

The phenomena of the cold welding could be inhibited with the addition of stearic acid as the PCA. In this case, the powder is not adhered together and powder morphology retains its lamellar structure. As cryomilling time increases, the thickness of the powder becomes smaller and smaller while the powder fragmentation and grain refinement continue to take place. Nevertheless, this kind of morphology is not suitable for cold spray process.

On the other hand, when PCA is not used in the cryomilling process, the lamellar powder particles are welded together by hydrostatic pressure and the morphology of the powder particles transforms into equiaxed polygonal structure. This kind of morphology has high flowability and excellent drag coefficient [37]. Therefore, it is very suitable for CS process to achieve high kinetic energy.

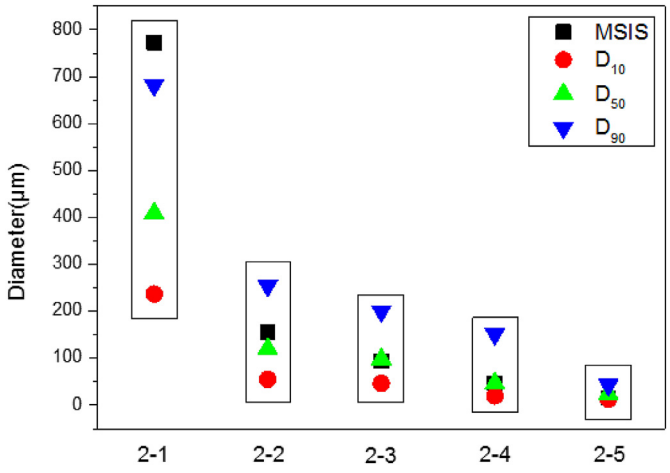

Fig. 7. Comparison of particle size and MSIS size distribution in case when PCA was not used in the milling chamber.

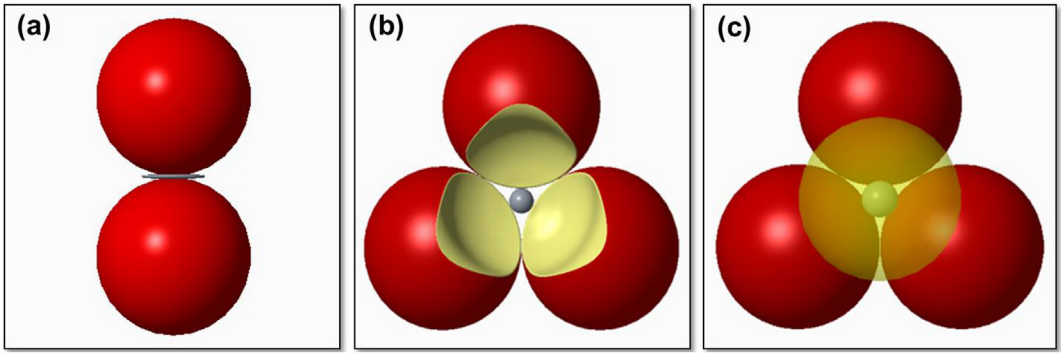

Fig. 6. Schematic representation of (a) first fragmentation mechanism, (b) second fragmentation mechanism at MSIP and (c) powder morphology controlling mechanism at MSIS.

Table 2
The interstitial hole diameter (μm) of all possible interstices formed in the milling pot for sample 2–5.

Interstice forming media	Tetrahedral interstice		Rectangular pyramid interstice		Octahedral interstice	
	Combination	Hole size (μm)	Combination	Hole size (μm)	Combination	Hole size (μm)
$D_{0.1}$ & Pot wall	($3 \times D_{0.1}$ & Pot wall)	33.33	($4 \times D_{0.1}$ & Pot wall)	50		
$D_{0.1}$ & D_{10}	($3 \times D_{0.1}$ & D_{10})	33.11	($4 \times D_{0.1}$ & D_{10})	49.76	–	–
$D_{0.1}$ & D_7	($3 \times D_{0.1}$ & D_7)	33.02	($4 \times D_{0.1}$ & D_7)	49.66		
$D_{0.1}$ & D_5	($3 \times D_{0.1}$ & D_5)	32.9	($4 \times D_{0.1}$ & D5)	49.52		
$D_{0.1}$ & $D_{0.1}$	($4 \times D_{0.1}$)	22.5	–		($6 \times D_{0.1}$)	41.4

4.2. Distribution of Particle size without PCA

As described above, in case when PCA is not used during cryomilling, the distribution of particle size is easy to be controlled by vibration milling because of the dominance of second fragmentation mechanism over cold welding mechanism (first type of fragmentation mechanism). The size of the milled powder depends on size distribution of various kinds of interstices formed by the grinding media. The probability of tetrahedral interstices (Fig. 6(c)) generated by smallest balls to form minimum size interstice in solid space (MSIS), is the highest during milling process. As a result, the final particle size distribution approaches the MSIS distribution. This implies that MSIS controls the geometrical characteristics of the powder in the whole cryomilling process. By comparing the distribution of particle size with MSIS, it can be noticed that there is a perfect fit between D_{50} of particle size and MSIS, for the value of MSIS lower than 100 μm (Fig. 7). However, with increasing MSIS, D_{50} of particle size is gradually decreased compared with the value of minimum sized interstice. The reason for this phenomenon is possibly due to the following factors. Firstly, in the cryomilling process, most of the powder particles are filled into the interstices, and with the passage of time, the powder particles are severely deformed and cold welded with each other. Consequently, the distribution of the particle size arrives closer to the distribution of interstice size. Secondly, in case of using larger size grinding media, the interstice space also gets bigger. However, to deform and cold weld bigger particles, more energy is required. Therefore, it is more difficult to cryomill bigger particles than the smaller ones. Meanwhile, with the consumption of powder with smaller size, only few milled fragments could be used in the cold welding process. Consequently, the increase in powder size distribution becomes slower and slower with milling time or even tends to stop. Therefore, the particle size distribution of powder 2–1 is lower than the minimum interstice size.

Table 2 presents the summary of all theoretically possible interstices, along with the diameter of their interstitial hole, formed during the milling process of powder 2–5. The possible interstices are tetrahedral, octahedral and rectangular pyramid. However, the probability of forming rectangular pyramid interstice and octahedral interstice is much less than the likelihood of the tetrahedral interstice. That is why the D_{90} of powder 2–5 is of the order of ~43 μm.

From above discussion, following inferences could be drawn about the particle size distribution, (a) when the cryomilling process arrives at dynamic equilibrium, all of the grinding media and the powder assume close packed structure viz. the smaller particles and milling media fill in the interstices formed by the larger milling balls. (b) Under dynamic equilibrium, it is assumed that the probability of locating each type of ball at a particular place in the pot is constant. However, this probability would not be similar at different locations of the milling pot. In other words, each type of the grinding media might have uneven or gradient distribution within the pot. This is closely related to the following factors; (a) the geometrical parameters of the milling pot, (b) the size and the density of the grinding media and (c) the amplitude and frequency of the cryomilling system. Hence, closed packed arrangement of various kinds of balls would almost remain same at each mode of vibration. Therefore, it can be deduced that the probability of the type and the size distribution of the interstice in every vibration period remains constant. This is only a function of quantity and size distribution of the grinding media. Therefore, it is reasonable to assume that the distribution of particle size is a function of MSIS size distribution, which mainly depends on the size distribution of the grinding media.

5. Conclusion

1. In this study, nanostructured Al powder was successfully produced by using modified pot vibration milling. The grains of pure Al powder were progressively refined with increase in milling time.
2. The main mechanism of vibration milling is double-impact by the grinding media which result in compressive deformation of powder particles in each vibration period.
3. When the powder particle is located in the middle of two grinding media, it experiences uniaxial compression, and deforms severely into lamellar structure fragments. This is the main process of grain refinement of powder as well as the first mechanism of powder fragmentation.
4. In case, the powder is located within the interstices of the grinding media, it is compressed hydrostatically. If the size of powder is bigger than MSIP, the powder is broken down into small particles due to intense compressive forces. This could be considered as the second fragmentation mechanism of the powder.
5. In case, PCA is used in the milling process, cold welding process could be inhibited and the morphology of powder assumes lamellar structure. In contrast, when PCA is not used in the milling process, the powder assumes equiaxed polygonal morphology. The particle size distribution and geometrical characteristic of polygonal powder is mainly controlled by the interstice size distribution (i.e. MSIS) of the milling media.

Acknowledgement

Financial support from National Natural Science Foundation of China through Grant No. 51671205 is highly acknowledged.

References

[1] H. Gleiter, Nanocrystalline materials, Prog. Mater. Sci. 33 (4) (1989) 223–315.
[2] G. Cao, Nanostructures and Nanomaterials: Synthesis, Properties and Applications, second ed. Imperial College Press, London, 2004.
[3] Y. Wang, M. Chen, F. Zhou, E. Ma, High tensile ductility in a nanostructured metal, Nature 419 (6910) (2002) 912–915.
[4] P.V. Liddicoat, X.Z. Liao, Y. Zhao, Y. Zhu, M.Y. Murashkin, E.J. Lavernia, R.Z. Valiev, S.P. Ringer, Nanostructural hierarchy increases the strength of aluminium alloys, Nat. Commun. 1 (2010) 63.
[5] D. Liu, Y. Xiong, P. Li, Y. Lin, F. Chen, L. Zhang, J.M. Schoenung, E.J. Lavernia, Microstructure and mechanical behavior of NS/UFG aluminum prepared by cryomilling and spark plasma sintering, J. Alloys Compd. 679 (2016) 426–435.
[6] C. Koch, The Synthesis and Structure of Nanocrystalline Materials Produced by Mechanical Attrition: A Review, Vol. 2, 1993 109.
[7] P.H. Shingu, B. Huang, S.R. Nishitani, S. Nasu, Nano-meter order crystalline structures of Al-Fe alloys produced by mechanical alloying, Mater. Trans. 29 (1988) 3–10 Suppl.
[8] F. Zhou, J. Lee, S. Dallek, E.J. Lavernia, High grain size stability of nanocrystalline Al prepared by mechanical attrition, J. Mater. Res. 16 (12) (2001) 3451–3458.
[9] D.B. Witkin, E.J. Lavernia, Synthesis and mechanical behavior of nanostructured materials via cryomilling, Prog. Mater. Sci. 51 (1) (2006) 1–60.

[10] B.J.M. Aikin, R.M. Dickerson, D.T. Jayne, S. Farmer, J.D. Whittenberger, Formation of aluminum nitride during cryomilling of Nial, Scr. Met. Mater. 30 (1) (1994) 119–122.
[11] B.L. Huang, J. Vallone, C.F. Klein, M.J. Luton, Insitu synthesis of particle dispersed nanocrystalline nial by cryomilling, Intermetall. Matrix Composit. II 273 (1992) 171–176.
[12] R.J. Perez, B. Huang, E.J. Lavernia, Thermal stability of nanocrystalline Fe-10 wt.% Al produced by cryogenic mechanical alloying, Nanostruct. Mater. 7 (5) (1996) 565–572.
[13] M.L. Lau, B. Huang, R.J. Perez, S.R. Nutt, E.J. Lavernia, Synthesis and characterization of nanocrystalline M50 steel powders by cryomilling, Metastable Phases Microstruct. 400 (1996) 43–48.
[14] B. Huang, R.J. Perez, P.J. Crawford, A.A. Sharif, S.R. Nutt, E.J. Lavernia, Mechanically induced crystallization of Metglas Fe78b13si9 during cryogenic high-energy ball-milling, Nanostruct. Mater. 5 (5) (1995) 545–553.
[15] V.L. Tellkamp, A. Melmed, E.J. Lavernia, Mechanical behavior and microstructure of a thermally stable bulk nanostructured Al alloy, Metall. Mater. Trans. A 32 (9) (2001) 2335–2343.
[16] S.S. Li, J.L. Li, W. Li, Y.C. Xiong, Synthesis of nanocrystalline 7050 aluminium alloy powder by cryomilling, Rare Metal Mater. Eng. 41 (2012) 761–764.
[17] J. Ye, B.Q. Han, Z. Lee, B. Ahn, S.R. Nutt, J.M. Schoenung, A tri-modal aluminum based composite with super-high strength, Scr. Mater. 53 (5) (2005) 481–486.
[18] Q. Hou, Z.C. Shi, R.H. Fan, L.C. Ju, Cryomilling and characterization of metal/ceramic powders, High-Performance Ceramics VII, Pts 1 and 2, 512-515, 2012, pp. 127–131.
[19] V.L. Tellkamp, E.J. Lavernia, Processing and mechanical properties of nanocrystalline 5083 Al alloy, Nanostruct. Mater. 12 (1–4) (1999) 249–252.
[20] F. Tang, M. Hagiwara, J.M. Schoenung, Formation of coarse-grained inter-particle regions during hot isostatic pressing of nanocrystalline powder, Scr. Mater. 53 (6) (2005) 619–624.
[21] F. Tang, A. Hagiwara, J.A. Schoenung, Microstructure and tensile properties of bulk nanostructured Al-5083/SiCp composites prepared by cryomilling, Mat. Sci. Eng. A-Struct. 407 (1–2) (2005) 306–314.
[22] D.M. Liu, Y.H. Xiong, P. Li, Y.J. Lin, F. Chen, L.M. Zhang, J.M. Schoenung, E.J. Lavernia, Microstructure and mechanical behavior of NS/UFG aluminum prepared by cryomilling and spark plasma sintering, J. Alloys Compd. 679 (2016) 426–435.
[23] J.S. Cheng, H. Cui, H.B. Chen, B. Yang, J.Z. Fan, J.S. Zhang, Bulk nanocrystalline Al prepared by cryomilling, J. Univ. Sci. Technol. B 14 (6) (2007) 523–528.
[24] F. Tang, C.P. Liao, B. Ahn, S.R. Nutt, J.M. Schoenung, Thermal stability in nanostructured Al-5083/SiCp composites fabricated by cryomilling, Powder Metall. 50 (4) (2007) 307–312.
[25] J. Karthikeyan, 4 – The advantages and disadvantages of the cold spray coating process, Cold Spray Materials Deposition Process 2007, pp. 62–71.
[26] L. Ajdelsztajn, B. Jodoin, G.E. Kim, J.M. Schoenung, Cold spray deposition of nanocrystalline aluminum alloys, Metall. Mater. Trans. A 36a (3) (2005) 657–666.
[27] L. Ajdelsztajn, B. Jodoin, J.M. Schoenung, Synthesis and mechanical properties of nanocrystalline Ni coatings produced by cold gas dynamic spraying, Surf. Coat. Technol. 201 (3–4) (2006) 1166–1172.
[28] Y.Y. Zhang, J.S. Zhang, Recrystallization in the particles interfacial region of the cold-sprayed aluminum coating: strain-induced boundary migration, Mater. Lett. 65 (12) (2011) 1856–1858.
[29] Y.Y. Zhang, X.K. Wu, H. Cui, J.S. Zhang, Cold-spray processing of a high density nanocrystalline aluminum alloy 2009 coating using a mixture of As-atomized and As-cryomilled powders, J. Therm. Spray Techn. 20 (5) (2011) 1125–1132.
[30] L. Ajdelsztajn, A. Zúñiga, B. Jodoin, E.J. Lavernia, Cold-spray processing of a nanocrystalline Al—Cu—Mg—Fe—Ni alloy with Sc, J. Therm. Spray Techn. 15 (2) (2006) 184–190.
[31] A.C. Hall, L.N. Brewer, T.J. Roemer, Preparation of aluminum coatings containing homogenous nanocrystalline microstructures using the cold spray process, J. Therm. Spray Techn. 17 (3) (2008) 352–359.
[32] V.K. Champagne, M. Trexler, Y. Sohn, G.E. Kim, Novel cold spray nanostructured aluminum, Proceedings of the 13th International Conference on Aluminum Alloys (Icaa13) 2012, pp. 993–998.
[33] P. Richer, B. Jodoin, L. Ajdelsztain, E.J. Lavernia, Substrate roughness and thickness effects on cold spray nanocrystalline Al-Mg coatings, J. Therm. Spray Techn. 15 (2) (2006) 246–254.
[34] R. Ghelichi, S. Bagherifard, D. Mac Donald, M. Brochu, H. Jahed, B. Jodoin, M. Guagliano, Fatigue strength of Al alloy cold sprayed with nanocrystalline powders, Int. J. Fatigue 65 (2014) 51–57.
[35] M. Yandouzi, A.J. Bottger, R.W.A. Hendrikx, M. Brochu, P. Richer, A. Charest, B. Jodoin, Microstructure and mechanical properties of B4C reinforced Al-based matrix composite coatings deposited by CGDS and PGDS processes, Surf. Coat. Technol. 205 (7) (2010) 2234–2246.
[36] D.J. Woo, J.P. Hooper, S. Osswald, B.A. Bottolfson, L.N. Brewer, Low temperature synthesis of carbon nanotube-reinforced aluminum metal composite powders using cryogenic milling, J. Mater. Res. 29 (22) (2014) 2644–2656.
[37] B. Jodoin, L. Ajelsztajn, E. Sansoucy, A. Zúñiga, P. Richer, E.J. Lavernia, Effect of particle size, morphology, and hardness on cold gas dynamic sprayed aluminum alloy coatings, Surf. Coat. Technol. 201 (2006) 3422–3429.